

## Accurate Rydberg Excitations from the Local Density Approximation

Adam Wasserman,<sup>1</sup> Neepa T. Maitra,<sup>2</sup> and Kieron Burke<sup>1</sup>

<sup>1</sup>*Department of Chemistry and Chemical Biology, Rutgers University, 610 Taylor Road, Piscataway, New Jersey 08854, USA*

<sup>2</sup>*Department of Physics and Astronomy, Hunter College of the City University of New York,  
695 Park Avenue, New York, New York 10021, USA*

(Received 2 June 2003; published 29 December 2003)

Despite the incorrect asymptotic behavior of its potential, the time-dependent local density approximation can yield accurate optical spectra. The oscillator strengths of Rydberg excitations appear in the calculated spectrum as continuum contributions with excellent optical intensity. We explain why, illustrate this for the neon and helium atoms, and also discuss when such calculations of the optical response will be inaccurate.

DOI: 10.1103/PhysRevLett.91.263001

PACS numbers: 31.15.Ew, 31.10.+z, 31.25.Jf, 32.70.Cs

Density functional theory [1,2] has seen tremendous success in predicting ground-state properties of atoms, molecules and solids. Time-dependent density-functional theory (TDDFT) [3] allows application of density-functional methods to time-dependent problems. In the linear response regime [4,5], TDDFT predicts electronic transition frequencies and optical spectra of these systems (see Ref. [6] for examples). In Casida's matrix formulation [5], first the self-consistent solution of the ground-state KS equations is found. Transitions between occupied and unoccupied KS orbitals may then be regarded as a first approximation to the true excitations of the system. In a second step, these KS frequencies and optical intensities are corrected to become the true transitions of the many-body system.

Although the local density approximation (LDA) and generalized gradient approximation (GGA) yield useful approximations to the total energy of an atom or molecule, their corresponding ground-state KS potentials are poor approximations [7] to the exact one. In particular, the LDA (or GGA) potential decays exponentially at large distances, rather than as  $-1/r$  as the exact KS potential does. As a result, the LDA potential for an atom does not support a Rydberg series of bound states. The first ionization threshold in the optical spectrum is at the magnitude of the energy of the highest occupied atomic orbital (denoted HOMO): In an LDA or GGA calculation this is typically too small by several eV. These approximate potentials have excitations to the continuum at frequencies where Rydberg excitations occur in the exact potential. This led many researchers to believe that excitations into Rydberg states cannot be treated at all within LDA (or GGA), or that the only way to do so is by asymptotically correcting the potentials [8–12]. Exact exchange (OEP) potentials [13,14] decay correctly, but at significant additional computational cost.

Authors usually downplay the significance of their own results beyond the LDA threshold [15–18]. This prognosis is unnecessarily bleak. In fact, TDLDA yields accurate optical spectra, even near the ionization threshold. Fig-

ure 1 shows this for the neon atom. (Atomic units are used throughout.) The oscillator strengths associated with exact Rydberg excitations remain in the same frequency region in LDA (even though the Rydberg states themselves are missing), as suggested by Zangwill and Soven [19,20], and confirmed numerically by Zangwill [21] for the krypton atom, where the TDLDA *continuum* absorption in the range 10–14 eV was found to agree with the experimental *discrete* absorption within 5%. We explain why this is true for most atomic and molecular systems. In any calculation in which resolution of the Rydberg states is unimportant, TDLDA yields excellent approximate oscillator strengths.

First, consider the hydrogen atom potential,  $V(r) = -1/r$ . Now shift the potential upwards by a small amount  $C$ , and truncate it when it reaches zero, i.e.,

$$V_{\text{tr}}(r) = \begin{cases} -1/r + C, & r \leq 1/C, \\ 0, & r > 1/C. \end{cases} \quad (1)$$

Since this potential does not decay as  $-1/r$  at large distances, it does not support a Rydberg series. Its ionization potential is redshifted by about  $C$ . In Fig. 2, we plot

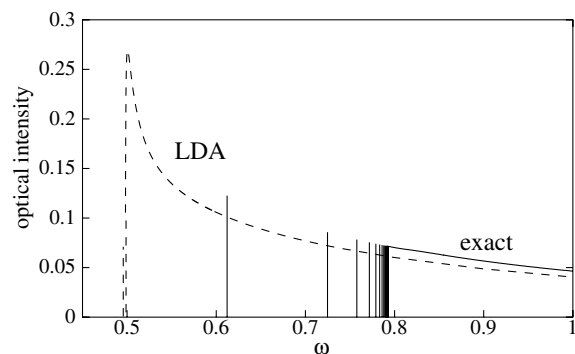


FIG. 1. Oscillator strengths (in inverse Hartrees) for the  $2p \rightarrow ns$  transitions in Ne as a function of photon energy (in Hartrees), from the exact KS potential, and from the LDA one. The discrete spectrum has been multiplied by the density-of-states factor (see text).

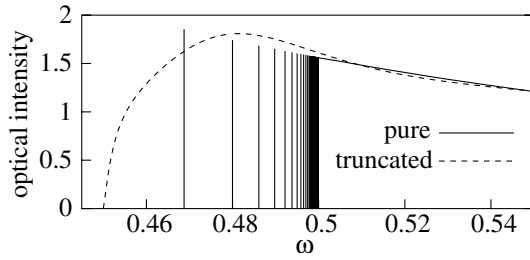


FIG. 2. Oscillator strengths (in inverse Hartrees) corresponding to  $1s \rightarrow np$  transitions (only shown for  $n \geq 4$ ) for a pure Coulomb and the truncated-Coulomb potential given by Eq. (1) with  $1/C = 20$ .

the optical intensity of both the pure and truncated Coulomb potentials in the vicinity of the ionization threshold, for  $C = 1/20$  (1.35 eV). The discrete transitions have optical intensity  $F_{fi} \delta(\omega - \omega_{fi})$ , where  $\omega_{fi}$  is the transition frequency and  $F_{fi}$  is its oscillator strength:

$$F_{fi} = \frac{2\omega_{fi}}{3} \frac{l_{>}}{2l_i + 1} \left[ \int_0^\infty dr \phi_f(r) r \phi_i(r) \right]^2. \quad (2)$$

Here  $\phi_i$  and  $\phi_f$  are the initial and final radial orbitals, and  $l_{>}$  is the larger of  $l_i$  and  $l_f$ . However, for reasons explained below, we represent them by single lines of height  $n^3 F_{fi}$ , where  $n$  is the radial quantum number of the final state. The similarity between the two curves is striking, both above the exact threshold and between the two ionization thresholds. As long as  $1/C$  is not too close to the nucleus, this behavior is observed for any value of  $C$ .

The phenomenon is well known in atomic physics [22]. The two potentials differ only by a constant, except at large  $r$  ( $> 1/C$ ). Their ground-state orbitals are virtually identical. The Rydberg states of the pure Coulombic potential are also almost identical to the *continuum* states of the shifted potential with the same transition frequency, unless they accidentally fall very close to the shifted potential's threshold. Thus the  $\langle \phi_f | r | \phi_i \rangle$  are about equal, except that states in the continuum are energy normalized. This produces a density of states factor,  $(dE/dn)^{-1}$ , where  $n$  is the final state index. In the case of a pure  $-1/r$  potential, this is simply  $n^3$ . Once this is accounted for, the optical response of the truncated potential is very close to that of the long-ranged potential.

Why is this phenomenon relevant to a TDLDA optical spectrum? Long ago, it was understood that the primary difference between LDA (or GGA) potentials and the exact KS potential is due to a lack of derivative discontinuity in the LDA potential [23]. This leads to the LDA XC potential differing from the exact XC potential by (nearly) a constant in the valence region: about  $(I + A)/2$  where  $I$  is the ionization potential and  $A$  the electron affinity. Taking  $I = 0.8$  and  $A \approx 0$  yields a shift of 0.4 as shown in Fig. 3. The variation of the difference with  $r$  is

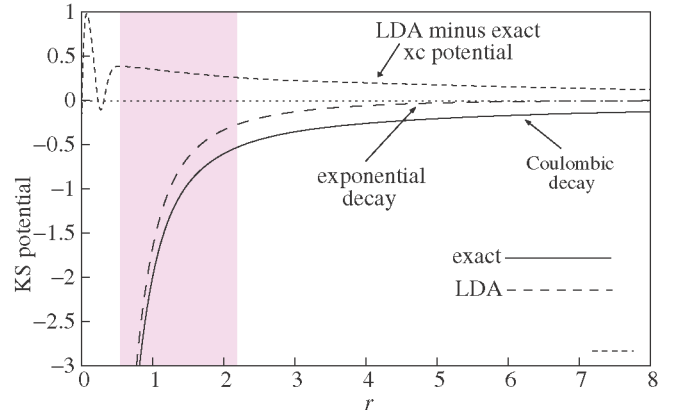


FIG. 3 (color online). Ne atom: the top curve shows the difference between the LDA and exact XC potential. The bottom curves show  $v_S^{\text{exact}}$  and  $v_S^{\text{LDA}}$ . In the valence region (shaded) the two potentials run almost parallel.

much smaller than that of the potentials in the valence region of the Ne atom.

To plot the Rydberg series of an exact KS potential, we write  $E_{nl} = -(n - \mu_{nl})^{-2}/2$ , where  $\mu_{nl}$  is the quantum defect, typically a very smooth function of  $n$ , and rapidly approaching a finite value as  $n \rightarrow \infty$ . To interpolate the  $n$  dependence of  $\mu$ , we used the same self-consistent interpolation of Al-Sharif *et al.* [24]. In practice,  $(dE/dn)^{-1}$  differs negligibly from  $(n - \mu_{nl})^3$  [22].

In Fig. 1, we plot the KS optical response spectrum for the Ne atom, for both the LDA and exact potentials. The LDA potential was obtained through a fully numerical self-consistent calculation [25]. The high quality of the LDA spectrum is already apparent in the bare KS spectrum (in the case of the Ne atom, the TDDFT corrections are small [26]); this is also true for the  $2s$ - $nd$  transitions (not shown). The LDA threshold is 0.3 (8 eV) below the exact threshold. Above the LDA threshold, the LDA oscillator strength is accurate to within 20% for all bound transitions. Table I shows this explicitly by extracting these from the height of the LDA curve at the exact transition frequencies. These LDA states are not resonances, but simple continuum states. From the table we see that LDA is accurate, even if not as accurate as OEP (the error from the latter is largely due to lack of correlation in the HOMO [27]). Thus, while not yielding an

TABLE I. Oscillator strengths for the first six discrete  $2p \rightarrow ns$  transitions in Ne.

Transition	LDA	OEP	Exact
$2p \rightarrow 3s$	2.22(-2)	2.84(-2)	2.70(-2)
$2p \rightarrow 4s$	3.74(-3)	4.43(-3)	4.46(-3)
$2p \rightarrow 5s$	1.32(-3)	1.54(-3)	1.57(-3)
$2p \rightarrow 6s$	6.22(-4)	7.15(-4)	7.34(-4)
$2p \rightarrow 7s$	3.42(-4)	3.91(-4)	4.03(-4)
$2p \rightarrow 8s$	2.09(-4)	2.37(-4)	2.45(-4)

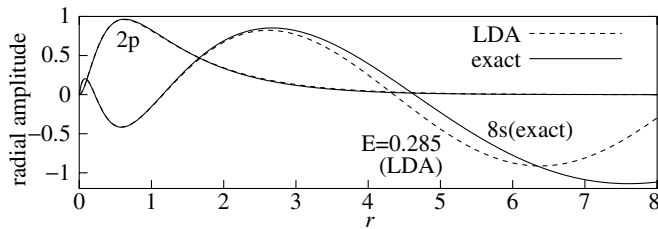


FIG. 4. Ne atom: LDA *continuum* state at energy  $E = 0.2853$ , and exact energy-normalized  $8s$  *bound* orbital, along with the LDA and exact  $2p$  orbitals.

approximation to the eigenvalues, accurate oscillator strengths are available from LDA (or GGA) if the exact transition frequencies are known.

The accuracy of the LDA spectrum is *not* a consequence of the Thomas-Reiche-Kuhn sum rule [22], which states that the total oscillator strength integrated over all frequencies gives a constant proportional to the number of electrons (we verified the satisfaction of this sum rule in all our calculations). After all, any one-body potential satisfies this. Rather, it is the detailed shape of the LDA KS potential that is important. LDA densities are close to exact densities, implying that occupied orbitals are quite accurate. In particular, the LDA HOMO ( $2p$  in this case), out of which we are computing the transitions, is almost identical to the exact HOMO (Fig. 4). This fact alone implies accurate behavior for the high-frequency limit of the optical spectrum. To see this, evaluate the dipole matrix element assuming the final state is a simple plane wave, as it will be when its energy is very high. One finds that

$$\int_0^\infty dr \phi_{E_s} r \phi_{2p} \xrightarrow{E \rightarrow \infty} -(3/2^{5/4}) Z \phi_{2p}''(r=0) E^{-11/4} / \sqrt{\pi}, \quad (3)$$

where  $Z$  is the nuclear charge. Thus an accurate HOMO near the nucleus yields accurate high-frequency behavior. Even at frequencies only slightly below the exact threshold, the final states are similar in regions that are significant for the optical response, and their different asymptotic behavior is irrelevant, as shown in Fig. 4.

We now discuss where the LDA response will *not* be accurate, namely, in the immediate vicinity of the LDA threshold. At this threshold, the LDA response incorrectly vanishes according to Wigner-threshold behavior [28]. How far above this value must one be to trust the accuracy of the LDA spectrum? To see this, we again truncate the Coulomb potential of Fig. 2 (where the truncation point was chosen appropriately for comparison purposes) but now choose a range of truncation values,  $r_0 = 20 \rightarrow 10$ , so that the threshold of the truncated spectrum,  $I_{tr}$ , passes through a discrete transition of the exact potential. Figure 5 shows that, as a discrete transition is absorbed into the continuum, its oscillator

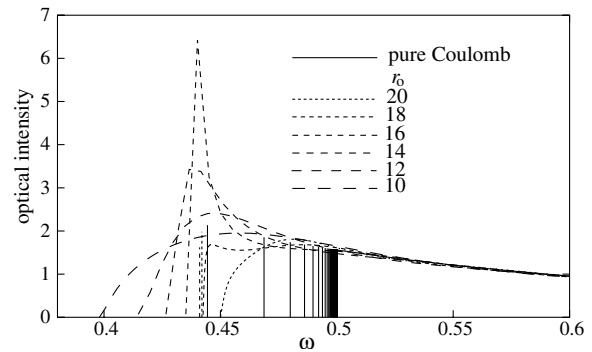


FIG. 5. The threshold of the truncated spectrum passes through the  $1s \rightarrow 3p$  discrete transition of the pure Coulomb potential as  $r_0$  goes from 18 to 16.

strength is at first a sharp peak centered on  $I_{tr}$ . When  $I_{tr}$  is well below the discrete transition, this peak has settled to an accurate envelope for that transition. Thus one can trust the truncated oscillator strength for all discrete transitions absorbed in the continuum except possibly the lowest. *Only* very close (within one transition on either side) to  $I_{tr}$  is the truncated spectrum inaccurate. In the case of Ne in Fig. 1, there is a barely bound transition (energy  $-2.3$  mH) in the LDA spectrum, whose oscillator strength has been partially absorbed by the continuum.

Finally, Fig. 6 shows both the bare KS response and the TDDFT corrected response of the He atom; the latter both exactly (from experiment and accurate quantum chemical calculations) and within TDLDA. These are the results of Stener *et al.* [29], but we do not shift the LDA spectrum to correct for the threshold error: we compare oscillator strengths at the same frequency, not energy. The TDDFT corrections are small, and overcorrect the bare LDA results, but clearly are consistent with our observations for the bare spectra.

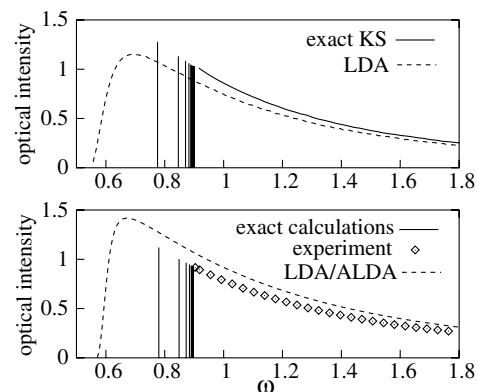


FIG. 6. He atom: The top panel shows the bare exact KS and LDA spectra, and the lower panel shows the TDDFT corrected spectra, LDA/ALDA results are from [29] but unshifted; the exact calculations are from [30], multiplied by the density of states factor (see text), and the experimental results are from [31]

Often the excited state *energy* is of primary interest, especially to quantum chemists focused on molecular spectroscopy. However, for many other properties, the integrated response is relevant. The dispersion forces between separated molecules are determined by the (imaginary) frequency integral of the dynamic polarizabilities of the individual species. Our results imply that even LDA should be an excellent approximation, as was found in Ref. [32], and more recently in Ref. [33] for finite distances.

Moreover, it can happen that a bound  $\rightarrow$  bound transition is shifted into the continuum by TDLDA, but if it remains strongly peaked, our analysis shows that the transition frequency and photoabsorption intensity for this transition can be trusted, even though the transition is now bound  $\rightarrow$  free. The  $\pi \rightarrow \pi^*$  transition in benzene is an example of this [18].

We thank Walter Kohn for helpful discussions, Cyrus Umrigar for the exact ground-state density and XC potential of the neon and helium atoms, and the authors of [29] for their numerical results. This work was supported by the Petroleum Research Fund and by NSF Grant No. CHE-9875091.

- 
- [1] P. Hohenberg and W. Kohn, Phys. Rev. **136**, B864 (1964).  
[2] W. Kohn and L. J. Sham, Phys. Rev. **140**, A1133 (1965).  
[3] E. Runge and E. K. U. Gross, Phys. Rev. Lett. **52**, 997 (1984).  
[4] M. Petersilka, U. J. Gossmann, and E. K. U. Gross, Phys. Rev. Lett. **76**, 1212 (1996).  
[5] M. E. Casida, in *Recent Developments and Applications in Density-Functional Theory*, edited by J. M. Seminario (Elsevier, Amsterdam, 1996).  
[6] N. T. Maitra, K. Burke, H. Appel, E. K. U. Gross, and R. van Leeuwen, in *Reviews in Modern Quantum Chemistry: A Celebration of the Contributions of R. G. Parr*, edited by K. D. Sen (World-Scientific, Singapore, 2002), Vol. II, pp. 1186–1225.  
[7] B. Y. Tong and L. J. Sham, Phys. Rev. **144**, 1 (1966).  
[8] F. Della Salla and A. Görling, J. Chem. Phys. **116**, 5374 (2002).  
[9] M. Grüning, O. V. Gritsenko, S. J. A. van Gisbergen, and E. J. Baerends, J. Chem. Phys. **116**, 9591 (2002).  
[10] R. van Leeuwen and E. J. Baerends, Phys. Rev. A **49**, 2421 (1994).  
[11] M. E. Casida and D. R. Salahub, J. Chem. Phys. **113**, 8918 (2000).  
[12] D. J. Tozer and N. C. Handy, Phys. Chem. Chem. Phys. **2**, 2117 (2000).  
[13] T. Grabo, T. Kreibich, S. Kurth, and E. K. U. Gross, in *Strong Coulomb Correlations in Electronic Structure: Beyond the Local Density Approximation*, edited by V. I. Anisimov (Gordon and Breach, Tokyo, 1998).  
[14] S. Kümmel and J. P. Perdew, Phys. Rev. Lett. **90**, 043004 (2003).  
[15] K. Yabana and G. F. Bertsch, Phys. Rev. B **54**, 4484 (1996).  
[16] A. Rubio, J. A. Alonso, X. Blase, L. C. Balbás, and S. G. Louie, Phys. Rev. Lett. **77**, 247 (1996).  
[17] I. Vasiliev, S. Ögüt, and J. R. Chelikowsky, Phys. Rev. Lett. **82**, 1919 (1999).  
[18] I. Vasiliev, S. Ögüt, and J. R. Chelikowsky, Phys. Rev. B **65**, 115416 (2002).  
[19] A. Zangwill and P. Soven, Phys. Rev. A **21**, 1561 (1980).  
[20] G. D. Mahan and K. R. Subbaswamy, *Local Density Theory of Polarizability* (Plenum Pub. Corp., New York, 1990).  
[21] A. Zangwill, in *Atomic Physics 8*, edited by I. Lindgren, A. Rosén, and A. Svanberg (Plenum, New York, 1983), p. 347.  
[22] H. Friedrich, *Theoretical Atomic Physics* (Springer, New York, 1991), Sec. 3.1.  
[23] J. P. Perdew, in *Density Functional Methods in Physics*, edited by R. M. Dreizler and J. da Providencia (Plenum, New York, 1985), p. 265.  
[24] A. I. Al-Sharif, R. Resta, and C. J. Umrigar, Phys. Rev. A **57**, 2466 (1998).  
[25] E. Engel and R. M. Dreizler, J. Comput. Chem. **20**, 31 (1999).  
[26] H. Appel, E. K. U. Gross, and K. Burke, Phys. Rev. Lett. **90**, 043005 (2003).  
[27] M. Petersilka, E. K. U. Gross, and K. Burke, Int. J. Quantum Chem. **80**, 534 (2000).  
[28] E. P. Wigner, Phys. Rev. **73**, 1002 (1948).  
[29] M. Stener, P. Decleva, and A. Görling, J. Chem. Phys. **114**, 7816 (2001).  
[30] A. Kono and S. Hattori, Phys. Rev. A **29**, 2981 (1984).  
[31] J. A. R. Samson, Z. X. He, L. Yin, and A. Haddad, J. Phys. B **27**, 887 (1994).  
[32] W. Kohn, Y. Meir, and D. E. Makarov, Phys. Rev. Lett. **80**, 4153 (1998).  
[33] A. J. Misquitta, B. Jeziorski, and K. Szalewicz, Phys. Rev. Lett. **91**, 033201 (2003).